



Assessment of Satellite-Based Chlorophyll-a Algorithms in Eutrophic Korean Coastal Waters: Jinhae Bay Case Study

Joo-Eun Yoon¹, Jae-Hyun Lim², SeungHyun Son³, Seok-Hyun Youn⁴, Hyun-Ju Oh⁴, Jae-Dong Hwang⁴, Jae-II Kwon⁵, Seong-Su Kim¹ and Il-Nam Kim^{1*}

¹ Department of Marine Science, Incheon National University, Incheon, South Korea, ² Fisheries Resources and Environment Division, East Sea Fisheries Research Institute, National Institute of Fisheries Science, Gangneung, South Korea, ³ CIRA, Colorado State University, Fort Collins, CO, United States, ⁴ Oceanic Climate and Ecology Research Division, National Institute of Fisheries Science, Busan, South Korea, ⁵ Marine Disaster Research Center, Korea Institute of Ocean Science and Technology, Busan, South Korea

OPEN ACCESS

Edited by:

Peng Liu,
Institute of Remote Sensing and
Digital Earth (CAS), China

Reviewed by:

Mukesh Gupta,
Instituto de Ciencias del Mar
(ICM), Spain

Gabriela Noemí Williams,
National Council for Scientific and
Technical Research
(CONICET), Argentina

*Correspondence:

Il-Nam Kim
ilnamkim@inu.ac.kr

Specialty section:

This article was submitted to
Environmental Informatics,
a section of the journal
Frontiers in Marine Science

Received: 11 June 2018

Accepted: 12 June 2019

Published: 28 June 2019

Citation:

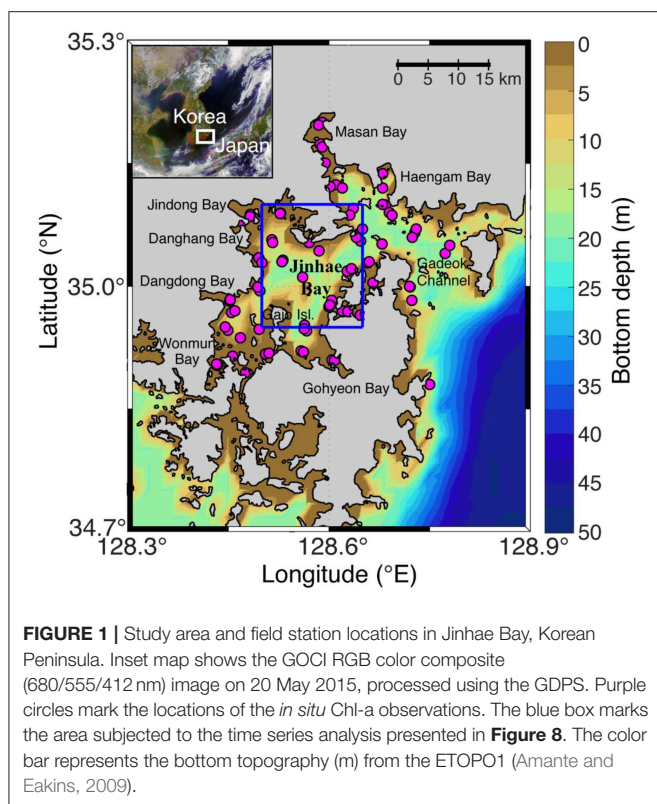
Yoon J-E, Lim J-H, Son S, Youn S-H, Oh H-J, Hwang J-D, Kwon J-I, Kim S-S and Kim I-N (2019) Assessment of Satellite-Based Chlorophyll-a Algorithms in Eutrophic Korean Coastal Waters: Jinhae Bay Case Study. *Front. Mar. Sci.* 6:359.
doi: 10.3389/fmars.2019.00359

Jinhae Bay, one of the most important aquaculture areas in Korean coastal waters, has suffered from serious environmental problems due to intensive anthropogenic activities since the 1970s. Determining the response of coastal ecosystems in Korea to anthropogenic activities requires understanding the characteristics of chlorophyll-a concentration (Chl-a), and the high spatiotemporal resolution of the Geostationary Ocean Color Imager (GOCl) can aid these efforts. However, producing reliable satellite-based Chl-a estimates is challenging in optically complex coastal waters and the Chl-a estimation algorithms must be assessed regionally. Based on *in situ* Chl-a measurements collected in Jinhae Bay between 2011 and 2016, we evaluated GOCl-derived Chl-a estimates obtained using six ocean color Chl-a algorithms: two standard open ocean algorithms, one GOCl-standard algorithm, and three Tassan's algorithms regionally modified for Korean waters. All of the algorithms tended to underestimate high Chl-a values $>0.9 \text{ mg m}^{-3}$. The Yellow Sea Large Marine Ecosystem Ocean Color Project (YOC) algorithm, one of the modified Tassan's algorithms, provided the best fit to the *in situ* Chl-a measurements in Jinhae Bay ($r = 0.51$, $p < 0.05$), including appropriate representations of the spatial and temporal variation. Therefore, this algorithm can be considered a baseline approach for satellite-based long-term coastal monitoring systems in Jinhae Bay.

Keywords: ocean color algorithm, coastal ecosystem, geostationary ocean color imager (GOCl), Korean waters, remote sensing

INTRODUCTION

Jinhae Bay, located on the southeastern coast of the Korean Peninsula, has shallow water depths ($<50 \text{ m}$) and weak tidal currents of $0.1\text{--}1 \text{ m s}^{-1}$ (Figure 1; Kang, 1991) and is the most important large-scale shellfish aquaculture production area in the Korean coastal waters (Lim et al., 2006; Bae et al., 2017). However, limited seawater exchange ($\leq 0.24 \text{ m s}^{-1}$) due to geographic complexity and



coastal freshwater discharge from heavy precipitation and streams, especially during summer, has led to the development of strong seasonal stratification (Cho et al., 2002; Kim S. Y. et al., 2012; Kim N. S. et al., 2016; Lee et al., 2018). The bay has also received the net influx of total suspended matter (TSM) from the Nakdong River through Gadeok channel (Park et al., 1995; Lee et al., 2006). In addition, water transparency, which is mainly determined by the magnitude of phytoplankton blooms and TSM discharges, has shown spatial variability on the average of ~ 3.7 m. In particular, the northeastern regions of Jinhae Bay (including Masan and Haengam Bays) showed lower value of ~ 2.3 m (i.e., relatively high turbidity condition), whereas the southwestern regions around Gajo Island exhibited higher value of ~ 4.9 m (i.e., relatively low turbidity condition; **Figure 1**; Cho et al., 1998; Ryu et al., 2018).

Since the 1970s, intensive anthropogenic activities in this area have discharged domestic sewage and land-use wastes (3,800 and 3,600 kg d⁻¹, respectively) into several inflowing streams (Lee et al., 2018), loading them with massive nutrient contents (Lee and Min, 1990). These characteristics have resulted in serious environmental problems, such as eutrophication, hypoxia, and harmful algal blooms (red tides), leading to significant changes in coastal biogeochemical cycles and ecosystem structures (Lee and Lim, 2006; Moon et al., 2008; Kim D. et al., 2012; Lee et al., 2017; Lim et al., 2018). Hence, coastal ecosystem conservation in this area has become an important socioeconomic and scientific issue, and there have been many calls for a coastal ecosystem monitoring and effective water quality management systems.

The Geostationary Ocean Color Imager (GOCCI), the world's first geostationary ocean color satellite, was launched in June 2010 to monitor short- and long-term changes in marine ecosystems around the Korean Peninsula (**Figure 1**; Cho et al., 2010). GOCCI provides ocean color products, such as remote sensing reflectance (R_{rs}), chlorophyll-a concentration (Chl-a), and TSM, in near real-time during the daytime, from 09:16 to 16:16 local time (a total of eight images per day), and at a high spatial resolution of 500 m (Ryu et al., 2011; Choi et al., 2012). The Chl-a product is widely used as a primary variable for water quality assessment because it is an indicator of phytoplankton biomass, which is an important component of all marine ecosystems (Vaiciute et al., 2012). Therefore, GOCCI-derived Chl-a can be monitored to track ecosystem dynamics and assess the temporal and spatial changes in coastal water quality around the Korean Peninsula in near real-time.

However, the estimation of Chl-a from ocean color satellites remains a challenging task in coastal waters, generally classified as Case-2 waters, where the optical properties are influenced not only by phytoplankton but also by other water constituents, such as TSM and/or colored dissolved organic matter (CDOM) (Morel and Prieur, 1977; Gordon and Morel, 1983; Tassan, 1994; Bukata et al., 1995; IOCCG, 2000; Ruddick et al., 2001; Pradhan et al., 2005; Siswanto et al., 2011; Tilstone et al., 2013). Therefore, a regionally optimized Chl-a algorithm must be applied to coastal waters by evaluating and tuning the Chl-a retrieval algorithms (Gitelson et al., 1996; Garcia et al., 2005; Hattab et al., 2013).

To date, several Chl-a algorithms have been developed and evaluated for Korean waters (Moon et al., 2010; Siswanto et al., 2011; Kim W. et al., 2016). The first validation of GOCCI-derived Chl-a estimates, based on the NASA global standard algorithms (O'Reilly et al., 2000) and regional algorithms developed for Korean waters (Moon et al., 2010; Siswanto et al., 2011), was performed using *in situ* data collected from near-shore coastal waters around the Korean Peninsula (Moon et al., 2012). This validation showed that these Chl-a algorithms were not suitable for Korean coastal waters because of the diverse bio-optical properties of these regions. Subsequently, Kim W. et al. (2016) evaluated the Chl-a estimates from GOCCI data obtained by applying newly derived coefficients of Chl-a algorithms for three turbidity levels, in reference to *in situ* data collected at 491 stations around the Korean Peninsula between 2010 and 2014. However, no Chl-a measurements from Jinhae Bay were involved in evaluation of the algorithms. Furthermore, no satellite-based study has yet focused on Jinhae Bay.

Therefore, the purpose of this study is to evaluate the GOCCI-derived Chl-a estimates for Jinhae Bay obtained by two global open ocean algorithms and four regional algorithms for Korean waters, in reference to *in situ* Chl-a measurements from 2011 to 2016. We aim to provide a baseline approach for a GOCCI-based long-term monitoring system that can produce accurate assessments and enable effective management of Jinhae Bay's coastal ecosystem and water quality, which is an area showing rapidly increasing anthropogenic activities.

DATA AND METHODS

In situ Data

Surface water samples (<1-m depth) were collected using a 5-L Niskin bottle (standard model 110, OceanTest Equipment Inc., <https://www.ocean testequip.com/>) with monthly to bi-monthly intervals between 2011 and 2016 at 54 stations in Jinhae Bay ($n = 1688$) as part of the coastal environmental monitoring program of the National Institute of Fisheries Science (NIFS), Korea (Figure 1). Chl-a samples were immediately collected by filtering 500-mL of surface seawaters onto 25-mm-diameter nitrocellulose filters. The filter papers were stored in the dark at -20°C before laboratory analysis. In the laboratory, Chl-a was extracted with 15-ml of 90% acetone for 24 h as described in EPA Method 445.0 (Knap et al., 1996; U.S. EPA., 1997a), and the Chl-a concentrations were then measured with a 10-AU fluorometer (Turner Designs, CA, USA; Welschmeyer, 1994). The fluorometer was calibrated with a standard Chl-a solution once a year and its calibration status was checked with the solid secondary standard material prior to each series of measurements. For the TSM analysis, 500-mL water samples were filtered through 47-mm-diameter GF/F filters, which were weighed prior to filtering and then reweighed after filtering and drying; the TSM was calculated as the difference between the initial and final weights. The diffuse attenuation coefficient (K_d) was derived from the Secchi depth, measured with a white 30-cm-diameter disk (Holmes, 1970). Salinity was determined from the conductivity and temperature readings by temperature/conductivity probe mounted on an YSI 6600 V2 Sonde (Yellow Springs Instruments, USA). Water sample for nitrate analysis was immediately filtered (0.45 μm , Millipore membrane syringe filter) directly into a vial and stored at -20°C . Nitrate was determined using the flow injection analysis system (QuAAstro, Seal Analytical) by cadmium reduction methods (U.S. EPA., 1997b). Total nitrogen was measured through determination of nitrate concentration after persulphate oxidation of non-filtered water sample (Grasshoff, 1983).

GOCI R_{rs} Data

GOCI L1B data (500 \times 500 m resolution), covering the time period and locations of the *in situ* measurements, were downloaded from the Korea Ocean Satellite Center (KOSC) website (<http://kosc.kiost.ac.kr>). These L1B images were processed to L2 R_{rs} data at six wavelength bands (412, 443, 490, 555, 660, and 680 nm) using the GOCI Data Processing System (GDPS, version 2.0), which implements the KOSC standard atmospheric correction algorithm. Only GOCI R_{rs} values acquired at 12:16 local time were used to avoid the influence of the solar zenith angle (Hooker and McClain, 2000).

Ocean Color Chl-a Algorithms

Six algorithms (two OCxS algorithms for the open ocean, one GOCI-standard algorithm, and three Tassan's algorithms regionally modified for Korean waters) were selected to assess the GOCI-derived Chl-a estimates in Jinhae Bay (Moon et al., 2010; NASA, 2010; Siswanto et al., 2011; Kim W. et al., 2016).

The OCxS algorithms were developed as the operational algorithms for NASA's Sea-Viewing Wide Field-of-view Sensor (SeaWiFS). They use a fourth-order polynomial relationship between the ratio of R_{rs} (i.e., blue-green band ratio) and Chl-a (NASA, 2010). In this study, we tested two OCxS algorithms: OC2S and OC3S.

OC2S uses the two-band ratio (NASA, 2010), given as

$$\text{Chl-a} = 10^{0.2511 - 2.0853R + 1.5035R^2 - 3.1747R^3 + 0.3383R^4}, \quad (1)$$

where

$$R = \log_{10} \frac{R_{rs}(490)}{R_{rs}(555)}. \quad (2)$$

OC3S uses the three-band ratio (NASA, 2010), given as

$$\text{Chl-a} = 10^{0.2515 - 2.3798R + 1.5823R^2 - 0.6372R^3 - 0.5692R^4}, \quad (3)$$

where

$$R = \log_{10} \frac{\max(R_{rs}(443), R_{rs}(490))}{R_{rs}(555)}. \quad (4)$$

As the regional algorithm for Korean waters, we first tested the GOCI-standard Chl-a algorithm, developed for GOCI products using *in situ* Chl-a data collected around the Korean Peninsula from 1998 to 2009 (Moon et al., 2010). The GOCI-standard is given as

$$\text{Chl-a} = 1.8528R^{-3.263}, \quad (5)$$

where

$$R = \frac{(R_{rs}(443) + R_{rs}(490)) - R_{rs}(412)}{R_{rs}(555)}. \quad (6)$$

Tassan's algorithm, developed for turbid waters (Tassan, 1994), was regionally optimized as the Yellow Sea Large Marine Ecosystem Ocean Color Project (YOC) algorithm, using *in situ* Chl-a measurements from the Yellow Sea and East China Sea acquired between 1998 and 2007 (Siswanto et al., 2011). The YOC algorithm is given as

$$\text{Chl-a} = 10^{0.342 - 2.511R - 0.277R^2}, \quad (7)$$

where

$$R = \log_{10} \frac{R_{rs}(443)}{R_{rs}(555)} \left[\frac{R_{rs}(412)}{R_{rs}(490)} \right]^{-1.012}. \quad (8)$$

Kim W. et al. (2016) modified Tassan's algorithm for the GOCI product by using *in situ* data (2010–2014) collected from coastal areas around the Korean Peninsula, East China Sea, and Tsushima Strait. This modification, termed Tassan-All, is given as

$$\text{Chl-a} = 10^{-0.0751 - 1.7156R - 0.1119R^2}, \quad (9)$$

where

$$R = \log_{10} \frac{R_{rs}(443)}{R_{rs}(555)} \left[\frac{R_{rs}(412)}{R_{rs}(490)} \right]^{-0.5093}. \quad (10)$$

Kim W. et al. (2016) also modified regionally the coefficients of Tassan's algorithm, applying different coefficients for three TSM levels: low TSM of $0\text{--}0.5 \text{ g m}^{-3}$ or $R_{rs}(555) < 0.004 \text{ sr}^{-1}$ (Tassan-LS); moderate TSM of $0.5\text{--}10 \text{ g m}^{-3}$ or $R_{rs}(555)$ of $0.004\text{--}0.015 \text{ sr}^{-1}$ (Tassan-MS); and high TSM of $>10 \text{ g m}^{-3}$ or $R_{rs}(555) > 0.015 \text{ sr}^{-1}$ (Tassan-HS). The three modifications are referred to collectively as the Tassan-TD algorithm.

The Tassan-LS algorithm is given as

$$\text{Chl-a} = 10^{-0.0509 - 1.6888R - 0.1497R^2}, \quad (11)$$

where

$$R = \log_{10} \frac{R_{rs}(443)}{R_{rs}(555)} \left[\frac{R_{rs}(412)}{R_{rs}(490)} \right]^{-0.4404}. \quad (12)$$

The Tassan-MS algorithm is given as

$$\text{Chl-a} = 10^{0.1235 - 1.6072R + 4.6815R^2}, \quad (13)$$

where

$$R = \log_{10} \frac{R_{rs}(443)}{R_{rs}(555)} \left[\frac{R_{rs}(412)}{R_{rs}(490)} \right]^{-1.0138}. \quad (14)$$

The Tassan-HS algorithm is given as

$$\text{Chl-a} = 10^{-0.2318 - 1.1292R + 2.6650R^2}, \quad (15)$$

where

$$R = \log_{10} \frac{R_{rs}(443)}{R_{rs}(555)} \left[\frac{R_{rs}(412)}{R_{rs}(490)} \right]^{-0.2307}. \quad (16)$$

Match-up Procedure

GOI R_{rs} values were extracted for a 5×5 -pixel window centered on the location of the *in situ* sample for comparison. The maximum temporal difference between the GOI and *in situ* measurements was set at 4 h. The following GOI L2 flags rendered a pixel invalid for the matching analysis: cloud or ice, land, atmospheric correction failure, unrealistic R_{rs} spectrum shape, out of GOI observation boundary, high solar zenith angle ($>70^\circ$), high satellite zenith angle ($>55^\circ$), cloud edge, bright pixel adjacency warning, Chl-a failure (not calculable), or Chl-a warning (Chl-a $>1,300 \text{ mg m}^{-3}$). The inter-slot radiometric discrepancy was not corrected in this study because this flag was not yet implemented in GDPS. We then calculated the mean and standard deviation (SD) of the 25 pixels and deleted those pixels with values outside the range of the mean $\pm 1.5 \text{ SD}$ (Bailey and Werdell, 2006). The mean R_{rs} value of all valid pixels within the 5×5 -pixel window was used for the comparisons. We accepted only matched pairs with mean R_{rs} values above zero at all six wavelength bands. The final number of matched pairs was 22.

Statistical Analysis

The performances of the tested algorithms were evaluated based on the following statistical parameters: Pearson's correlation coefficient (r), slope (S) and intercept (I) of Type-2 linear regression (York, 1966; Laws and Archie, 1981; Glover et al., 2011) fitted on log-transformed Chl-a data; root-mean-square error (RMSE, Δ); bias (δ); and mean ratio. The latter three parameters are defined, respectively, as

$$\Delta = \sqrt{\frac{1}{n} \sum_{i=1}^n (y_i - x_i)^2}, \quad (17)$$

$$\delta = \frac{1}{n} \sum_{i=1}^n (y_i - x_i), \quad (18)$$

and

$$\text{mean ratio} = \frac{1}{n} \sum_{i=1}^n \frac{y_i}{x_i}, \quad (19)$$

where x_i and y_i denote the *in situ* Chl-a data and corresponding GOI-derived Chl-a estimates for the i -th matched pair, respectively, and n is the number of matched pairs.

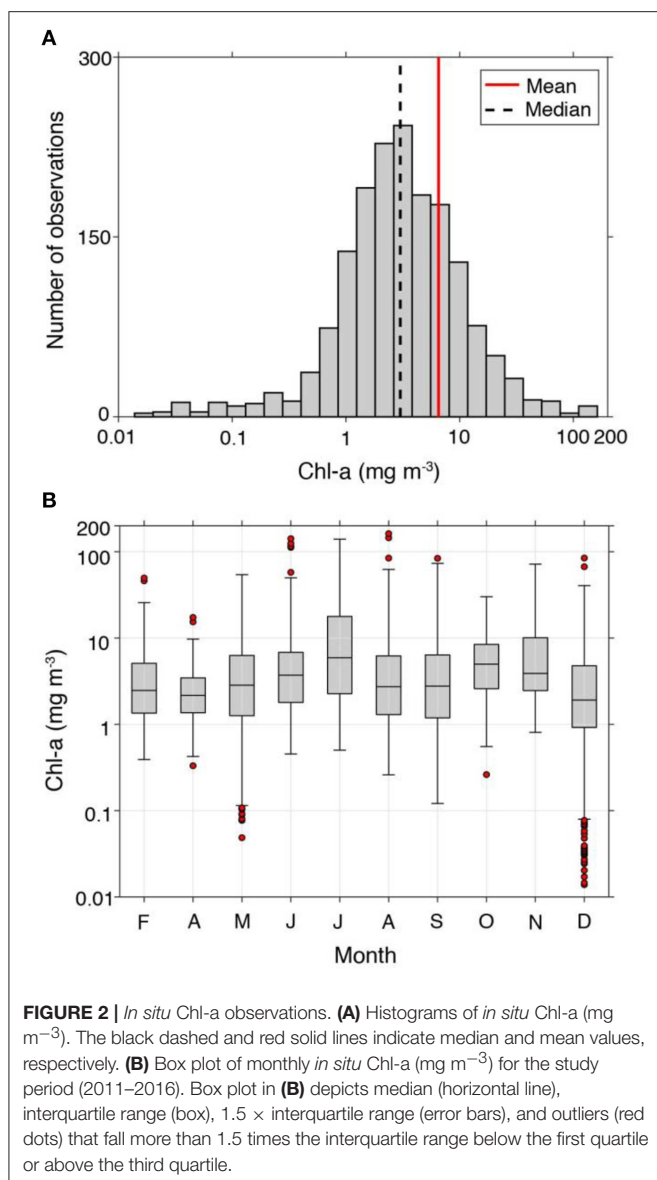
Outliers are defined as GOI-derived Chl-a estimates that fall outside the range from 1/20 to 20 times the *in situ* Chl-a. Outlier points were removed from the matching analysis for each algorithm (Pitarch et al., 2016).

RESULTS AND DISCUSSION

Spatiotemporal Variability of the Chlorophyll-a Measurements

The *in situ* Chl-a measurements ($n = 1688$), ranging between 0.014 mg m^{-3} and 162.1 mg m^{-3} , exhibited a log-normal distribution (Figure 2A). The median and mean values of Chl-a were 3.0 and 6.5 mg m^{-3} , respectively.

Chl-a was seasonally lower during the winter months (December and February; median value = 2.2 mg m^{-3}) and showed a gradually increasing trend in spring months (April and May; median value = 2.4 mg m^{-3} ; Figure 2B). The monthly mean Chl-a value was highest in July (mean \pm SD = $15.6 \pm 23.6 \text{ mg m}^{-3}$). Overall, the Chl-a values showed a positive correlation with the total nitrogen ($r = 0.5$, $p < 0.05$), whereas had a negative correlation with the salinity ($r = -0.4$, $p < 0.05$), which were collected from the same NIFS cruises during the study period (NIFS, 2012, 2013, 2014, 2015, 2016, 2017). This result indicates that the Chl-a dynamics in the Jinhae Bay were likely to be associated with the supply of nitrogen via low salinity waters. In particular, the maximum of monthly mean Chl-a values occurred in July 2011 ($31.5 \pm 30.9 \text{ mg m}^{-3}$; NIFS, 2012), corresponding to the highest nitrate concentration ($32.8 \pm 24.4 \mu\text{M}$) and the lowest salinity (18.0 ± 5.2) caused by heavy precipitation (<http://www.kma.go.kr/>). Previous studies reported that large phytoplankton blooms in Jinhae Bay occurred during the summer months (June through August) resulted from the high nutrient loadings associated with increased summer precipitation (accounting for $\sim 60\%$ of annual precipitation; Baek and Kim, 2010; Baek et al., 2012; Park et al., 2012; Kim et al.,



2013). These massive nutrient loadings have frequently caused outbreak of red tides in this area (Kwak et al., 2001). Seasonal secondary bloom occurred in October ($6.5 \pm 5.5 \text{ mg m}^{-3}$) as stratification became weak (Kim et al., 2015; Lim et al., 2018), and this bloom remained until November ($8.4 \pm 11.9 \text{ mg m}^{-3}$; Figure 2B). In December, Chl-a showed a seasonal minimum value (median value = 1.9 mg m^{-3}) with a large range from 0.014 to 84.5 mg m^{-3} .

The spatial distribution of monthly mean Chl-a values (Figure 3A) showed that relatively higher Chl-a concentrations occurred nearly all year in the northeastern regions of Jinhae Bay, where high nutrient loadings occur through a number of small streams proximate to industrial complexes and cities (Cho and Chae, 1998; Jeong et al., 2006), whereas relatively lower Chl-a concentrations were found in the southwestern regions (Kim et al., 2013, 2014; Lee et al., 2018). The seasonal and regional

Chl-a distribution patterns were similar to the TSM and K_d distributions, which also exhibited their highest values in July in the northeastern region of Jinhae Bay (Figure 3).

To determine whether light attenuation in Jinhae Bay was directly related to phytoplankton biomass, we analyzed the relationship between Chl-a and K_d , as well as between TSM and K_d . The K_d values were positively correlated with both TSM ($r = 0.4, p < 0.05, n = 1652$) and Chl-a ($r = 0.6, p < 0.05, n = 1684$; Figure 4), suggesting that the variability in light penetration in Jinhae Bay was determined not only by increases in phytoplankton biomass, but also by changes in TSM. A mean K_d value of 0.36 m^{-1} (range: $0.08\text{--}2.88 \text{ m}^{-1}$) was observed, which was similar to that of the coastal waters along the Gujarat coast and Gulf of Kachchh, India ($>0.15 \text{ m}^{-1}$; Sarangi et al., 2002). The TSM concentrations ranged from 0.6 to 72.8 g m^{-3} , with a mean value of 6.4 g m^{-3} ; this range was comparable to the ranges of moderate and high levels of TSM in the *in situ* datasets used to develop the Tassan-TD algorithm (Kim W. et al., 2016). These results indicate that Jinhae Bay represents the Case-2 waters, the optical properties of which are influenced by phytoplankton (Gordon and Morel, 1983; Bukata et al., 1995; IOCCG, 2000) and a number of other optical components (e.g., TSM).

Comparison of the Performance of Ocean Color Chl-a Algorithms

The atmospheric correction strategies applied can introduce large uncertainties and variability in remote sensing data from optically complex coastal waters (Gordon and Wang, 1994; IOCCG, 2000). For example, Siswanto et al. (2011) showed that the performance of the YOC algorithm as applied to the SeaWiFS data was relatively poor because of improper atmospheric corrections, based on a comparative analysis of the SeaWiFS and *in situ* R_{rs} data, whereas an improved atmospheric correction resulted in the improved performance of ocean color algorithms over coastal waters (Zhang et al., 2010; Siswanto et al., 2011). Kim W. et al. (2016) also reported that the overestimation of GOFCI R_{rs} in the blue bands (412, 443, and 490 nm), which is related to the atmospheric correction, may have caused underestimation of *in situ* Chl-a values $>1.5 \text{ mg m}^{-3}$ with moderate and high TSM levels.

In order to investigate the impact of the atmospheric correction algorithm on Chl-a estimates, therefore, we compared the R_{rs} data derived from the KOSC atmospheric correction algorithm with those derived from the NASA atmospheric correction algorithm for Jinhae Bay (Supplementary Text 1; Supplementary Figure 1). The comparison of the GOFCI R_{rs} values derived from the KOSC and NASA atmospheric correction algorithms, respectively, showed that the R_{rs} values at the blue bands were scattered more than those at the green band (555 nm; Supplementary Figure 1). The R_{rs} values at the blue bands derived from the NASA algorithm were lower than those derived from the KOSC algorithm, showing especially large biases in R_{rs} values at 412 nm. Although the development of KOSC atmospheric correction algorithm was based on the global NASA algorithm (Bailey et al., 2010), the KOSC algorithm has been partially updated for turbid Case-2 water corrections (Ahn et al.,

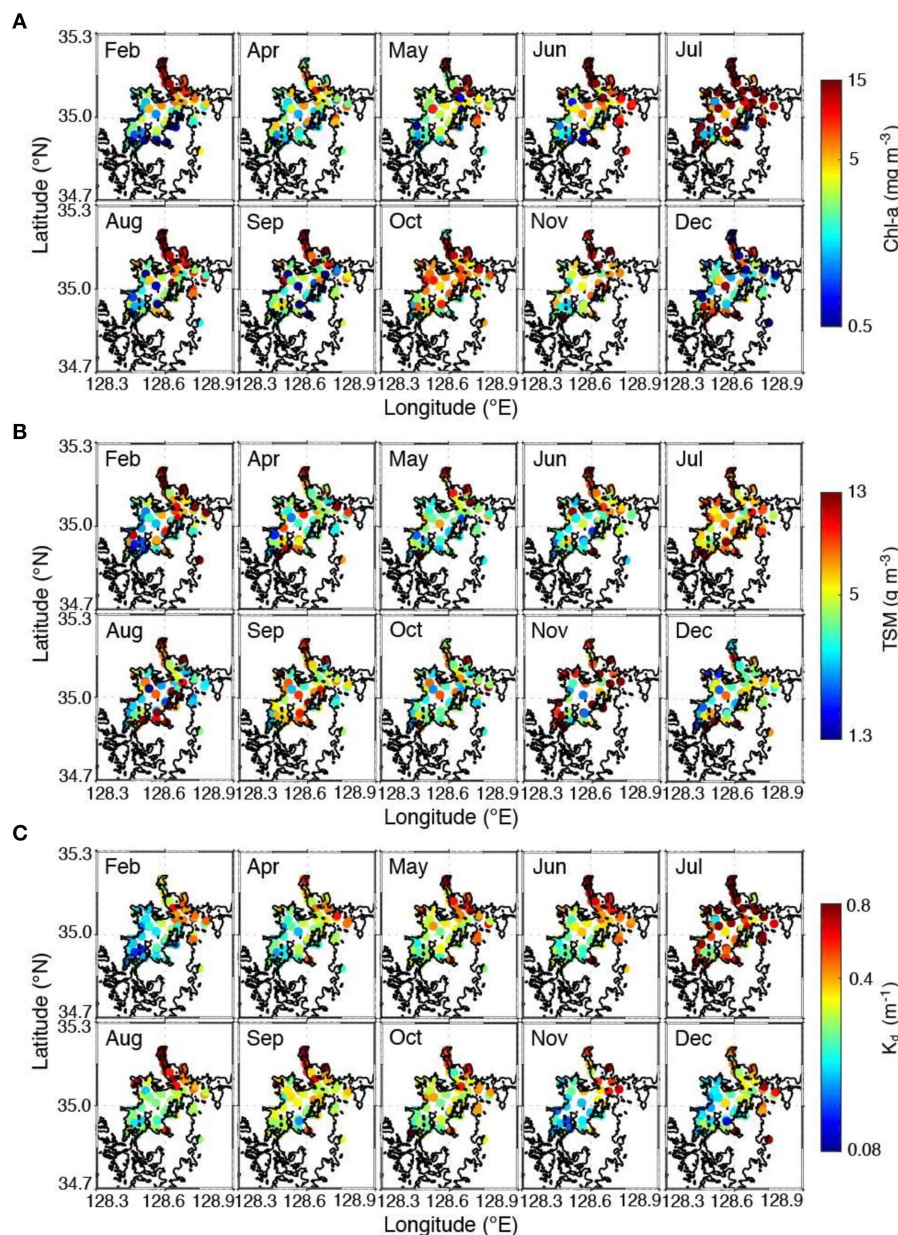


FIGURE 3 | Monthly spatial distribution of **(A)** *in situ* Chl-a (mg m^{-3}), **(B)** *in situ* TSM (g m^{-3}), and **(C)** *in situ* K_d (m^{-1}).

2012) and adjusted for vicarious calibration gains (Ahn et al., 2015) and aerosol correction schemes (Gordon and Wang, 1994; IOCCG, 2010; Ahn et al., 2016, 2018), indicating that the KOSC algorithm is likely to be more suitable to estimate local/regional Chl-a estimation in this study.

To evaluate the performances of the six ocean color Chl-a algorithms applied to the KOSC-GOCI R_s data from Jinhae Bay, we first constructed histograms of both the *in situ* and GOCI-derived Chl-a values in matched datasets (Figure 5). The distributions of the *in situ* and GOCI-derived Chl-a values both followed an approximately log-normal distribution. The GOCI-standard and YOC Chl-a algorithms showed similar ranges in

their Chl-a estimates relative to the corresponding *in situ* Chl-a values (Figures 5C,D). However, the histograms of the GOCI-derived Chl-a estimates obtained using the OC2S, OC3S, Tassan-All, and Tassan-TD Chl-a algorithms showed distributions shifted to the left, with relatively lower mean values for the Chl-a estimates (mean range: $0.7\text{--}1.0 \text{ mg m}^{-3}$) compared to the *in situ* Chl-a values ($2.7 \pm 1.9 \text{ mg m}^{-3}$; Figures 5A,B,E,F).

As shown in Figure 6, scatter plots of *in situ* Chl-a vs. GOCI-derived Chl-a estimates from the six ocean color Chl-a algorithms, most of the tested Chl-a algorithms overestimated the *in situ* Chl-a values ($<0.8 \text{ mg m}^{-3}$), except for Tassan-All. For high *in situ* Chl-a values ($>0.9 \text{ mg m}^{-3}$), the GOCI-derived

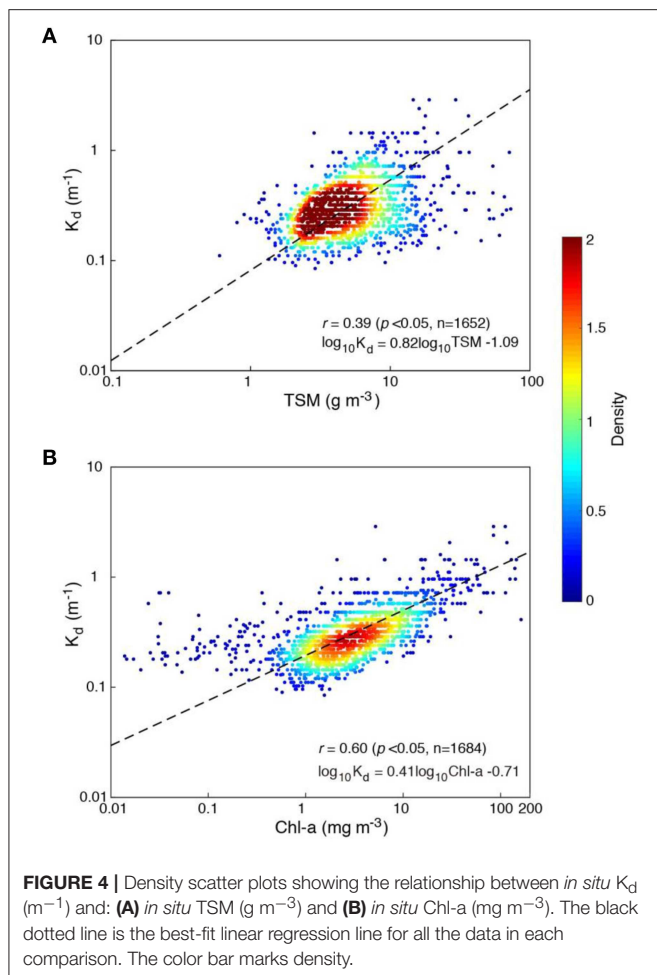


FIGURE 4 | Density scatter plots showing the relationship between *in situ* K_d (m^{-1}) and: **(A)** *in situ* TSM ($g\ m^{-3}$) and **(B)** *in situ* Chl-a ($mg\ m^{-3}$). The black dotted line is the best-fit linear regression line for all the data in each comparison. The color bar marks density.

Chl-a estimates from all algorithms generally underestimated the results. The GOCl-derived Chl-a values from the OC2S, OC3S, Tassan-All, and Tassan-TD algorithms ranged from 0.2 to 2.4 $mg\ m^{-3}$, compared to the high *in situ* Chl-a value range from 0.9 to 6.8 $mg\ m^{-3}$ (Figures 6A,B,E,F). This underestimation of high Chl-a values was comparable to the previously reported tendency of the Chl-a algorithm validation results from GOCl products for Korean coastal waters (Moon et al., 2010, 2012; Kim W. et al., 2016). However, overall the GOCl-derived Chl-a estimates from the YOC algorithm were distributed appropriately around the 1:1 line for *in situ* Chl-a values (Figure 6D) and also its mean ratio was close to one, indicating that the YOC algorithm yielded the most significant correlation ($r = 0.51$, $p < 0.05$) between the *in situ* and GOCl-derived Chl-a values (Table 1). Moreover, the YOC algorithm exhibited the bias ($\delta = 0.03$) closest to zero and a relatively low error ($\Delta = 2.52$), compared to the other algorithms. As a result of statistical analysis, the YOC algorithm performed best for the Jinhae Bay Chl-a estimations.

The performances of the Chl-a retrieval algorithms were also evaluated by comparing the spatial distributions of *in situ* and GOCl-derived Chl-a averages from two sampling periods, April 4–7, 2014 (Figure 7A) and August 3–4 and 6–7, 2016

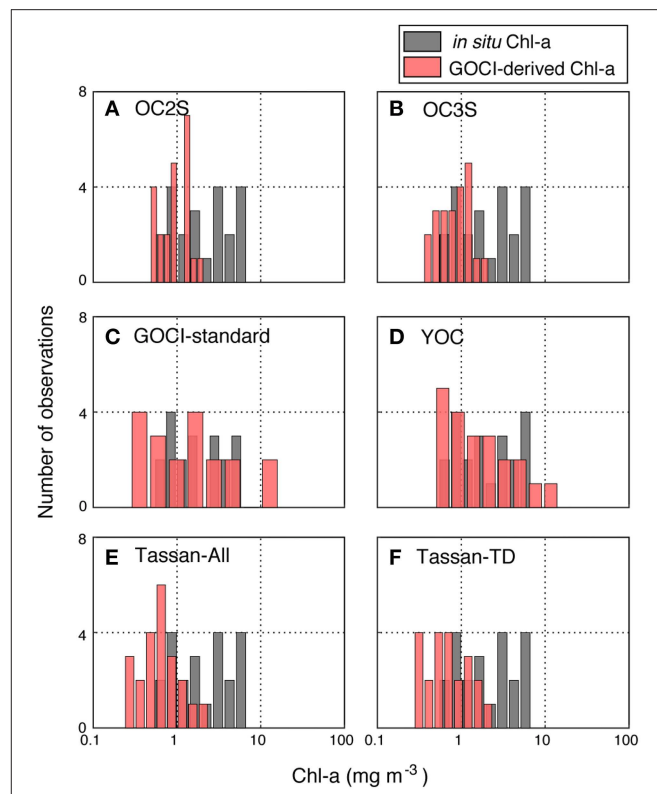


FIGURE 5 | Histograms of *in situ* Chl-a (gray bars) and GOCl-derived Chl-a obtained using the following six algorithms (red bars): **(A)** OC2S, **(B)** OC3S, **(C)** GOCl-standard, **(D)** YOC, **(E)** Tassan-All, and **(F)** Tassan-TD.

(Figure 7B). The spatial distributions of the GOCl-derived Chl-a values were calculated using the six Chl-a algorithms, excluding only low-quality pixels that were flagged as cloud or ice, land, atmospheric correction failure, unrealistic R_{rs} spectrum shape, out of GOCl observation boundary, high solar zenith angle ($>70^\circ$), high satellite zenith angle ($>55^\circ$), or cloud edge. Except for the GOCl-standard and YOC algorithms, all Chl-a algorithms tested estimated relatively lower Chl-a values compared to the *in situ* data, showing especially strong tendencies to underestimate Chl-a values for summer (August 3–4 and 6–7, 2016), when Chl-a concentrations were relatively higher. Although Chl-a estimates from the GOCl-standard algorithm showed a spatial distribution comparable to the *in situ* Chl-a values obtained for the spring period, the GOCl-standard algorithm overestimated the Chl-a values for the summer period when *in situ* Chl-a values were relatively higher than in the spring period. However, the *in situ* Chl-a averages from the two sampling periods both showed that spatial distribution patterns were similar to those estimated using the YOC algorithm, showing relatively higher values in areas near Gadeok Channel ($\sim 2\ mg\ m^{-3}$ in 2014 and $\sim 5\ mg\ m^{-3}$ in 2016, respectively) and relatively lower values around Gajo island ($\sim 1\ mg\ m^{-3}$ in 2014 and $\sim 2\ mg\ m^{-3}$ in 2016, respectively).

To further evaluate the accuracy of the YOC algorithm as applied to the Jinhae Bay data, the YOC algorithm was applied to GOCl R_{rs} data obtained over the 2011–2016 period. The

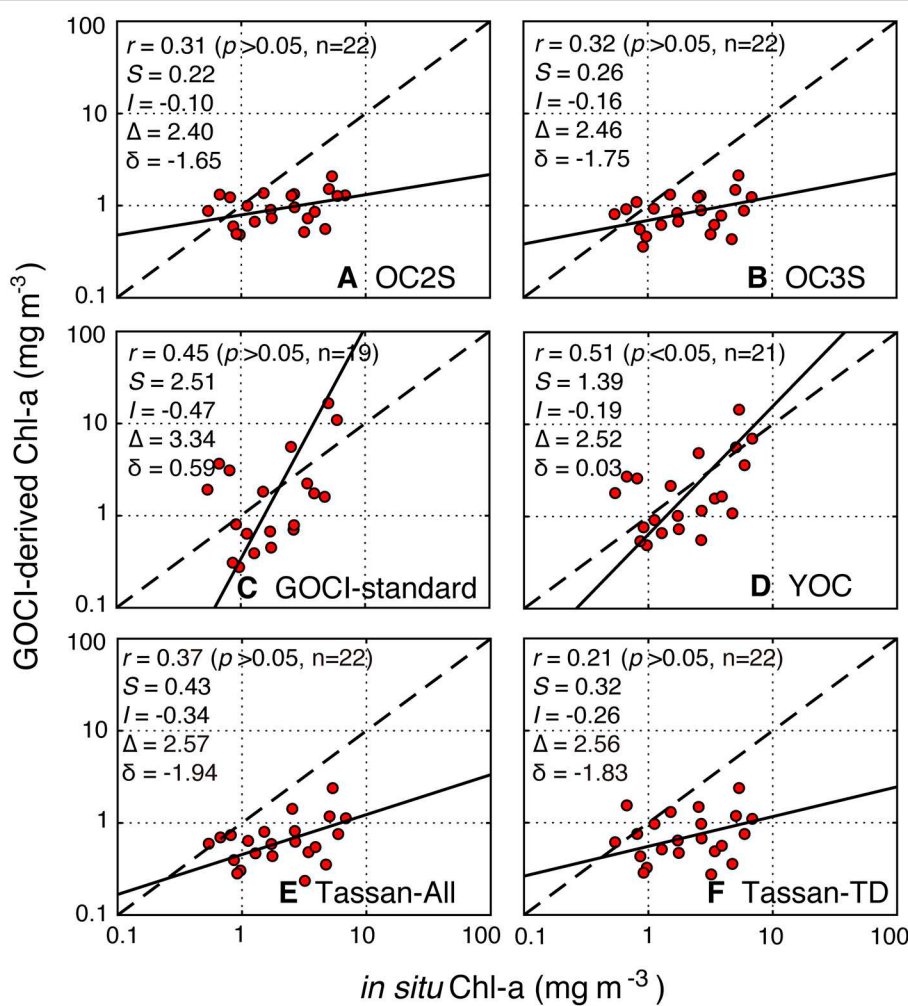


FIGURE 6 | Scatter plots between *in situ* Chl-a and GOCl-derived Chl-a for the six algorithms: **(A)** OC2S, **(B)** OC3S, **(C)** GOCl-standard, **(D)** YOC, **(E)** Tassan-All, and **(F)** Tassan-TD. The dashed and solid black line mark the 1:1 line and the Type-2 linear regression fit, respectively.

TABLE 1 | Statistical results for the matched pairs in Jinhae Bay.

Algorithm	r	p-value	S	I	δ	Δ	Mean ratio	n
OC2S	0.31	$p > 0.05$	0.22	-0.10	-1.65	2.40	0.60	22
OC3S	0.32	$p > 0.05$	0.26	-0.16	-1.75	2.46	0.53	22
GOCl-standard	0.45	$p > 0.05$	2.51	-0.47	0.59	3.34	1.39	19
YOC	0.51	$p < 0.05$	1.39	-0.19	0.03	2.52	1.21	21
Tassan-All	0.37	$p > 0.05$	0.43	-0.34	-1.94	2.57	0.40	22
Tassan-TD	0.21	$p > 0.05$	0.32	-0.26	-1.83	2.56	0.50	22

flags applied to this analysis were the same as those applied to the spatial analysis. Temporal patterns were analyzed based on the average value for the blue box area shown in **Figure 1** (34.95°N – 35.1°N and 128.5°E – 128.65°E). The area-averaged daily time series of *in situ* Chl-a values from 2011 to 2016 was compared with the GOCl-derived Chl-a values obtained using the YOC algorithm (**Figure 8**). The daily *in situ* Chl-a values

varied from 0.03 to 56.1 mg m^{-3} , whereas the GOCl-derived Chl-a values from YOC algorithm varied from 0.04 to 130.2 mg m^{-3} . The YOC algorithm generally slightly underestimated the Chl-a values compared to the *in situ* Chl-a values (**Figure 8**). Nonetheless, the slight discrepancies did not inhibit the YOC algorithm's reasonable representations of the seasonal variation of the *in situ* data.

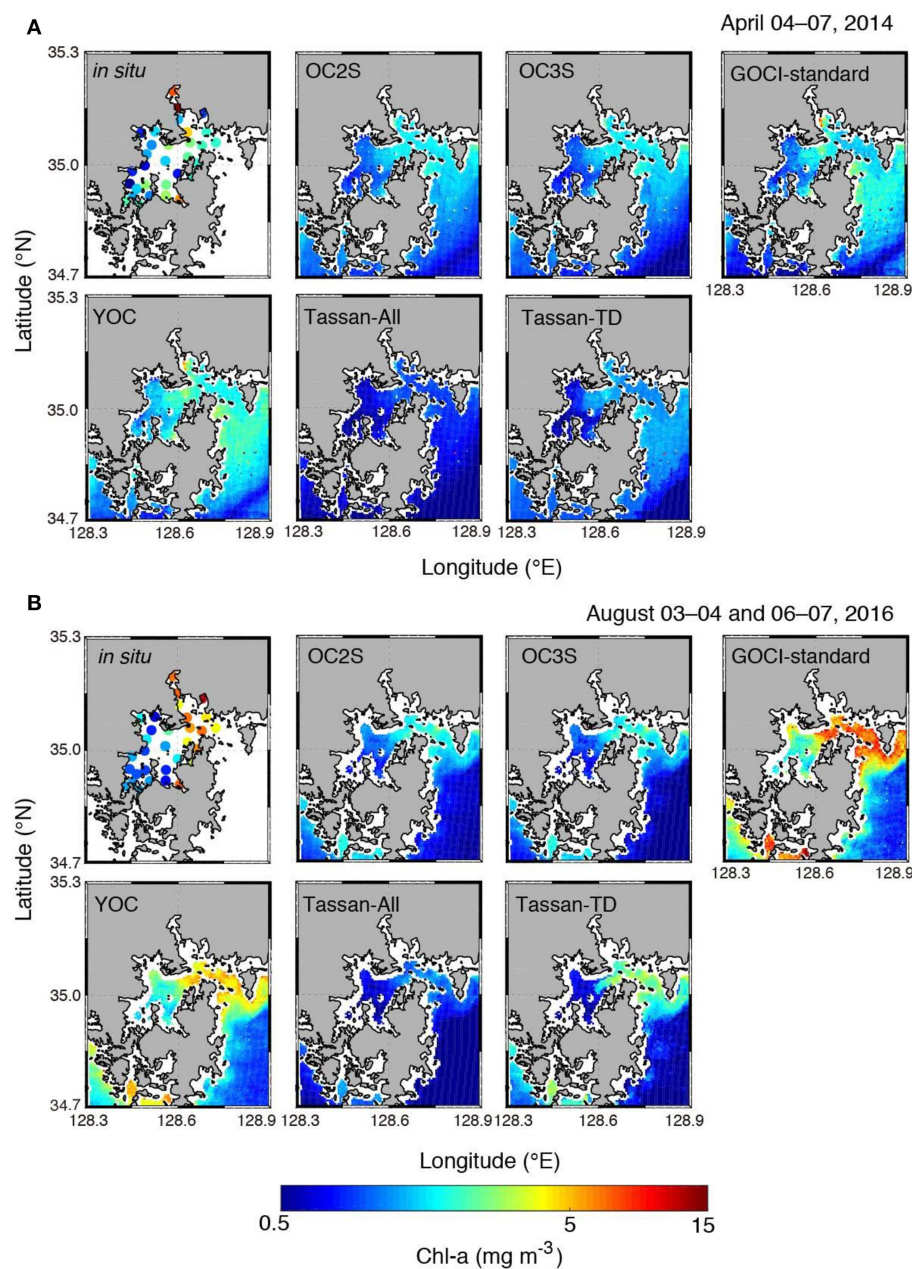


FIGURE 7 | Spatial distribution of *in situ* Chl-a (mg m^{-3}) and GOCl-derived Chl-a from six algorithms averaged for two sampling periods: **(A)** April 4–7, 2014 and **(B)** August 3–4 and 6–7, 2016, respectively. We excluded pixels with extreme concentrations (Chl-a $<0.001 \text{ mg m}^{-3}$ or Chl-a $>500 \text{ mg m}^{-3}$) and low-quality L2 data flagged as cloud or ice, land, atmospheric correction failure, unrealistic R_{rs} spectrum shape, out of GOCl observation boundary, high solar zenith angle ($>70^\circ$), high satellite zenith angle ($>55^\circ$), or cloud edge from the analysis.

In summary, the YOC algorithm showed a statistically significant correlation with *in situ* Chl-a values from Jinhae Bay (Figure 6D; Table 1). The spatial distribution of the GOCl-derived Chl-a estimates from the YOC algorithm was also closest to that of the *in situ* Chl-a values (Figure 7). Furthermore, the daily time series of the *in situ* Chl-a values was agreed well with the GOCl-derived Chl-a values obtained using YOC algorithm, showing the distinctive seasonal variations (Figure 8).

Therefore, the YOC algorithm will enable monitoring of ecosystem responses to anthropogenic impacts with near real time in the Jinhae Bay.

Suggestions for Future Research

In this study, the evaluation of the Chl-a algorithms was performed using only *in situ* Chl-a measurements, without considering *in situ* R_{rs} measurements from Jinhae Bay, which

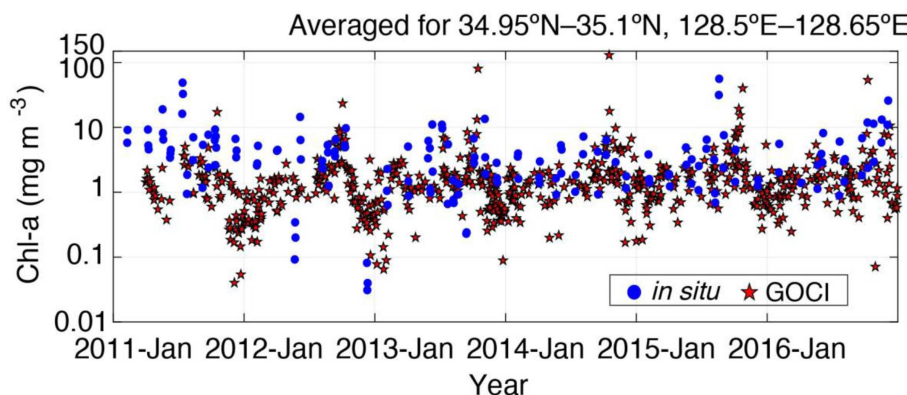


FIGURE 8 | Time series of the *in situ* Chl-a values (blue circles) and GOCI-derived Chl-a estimates from the YOC algorithm (red stars), averaged for the blue box area shown in **Figure 1** (34.95°N – 35.1°N and 128.5°E – 128.65°E). Pixel exclusion criteria were the same as in **Figure 7**.

inhibited the validation of the atmospheric correction and the development and assessment of a regionally optimized Chl-a algorithm based on *in situ* R_{rs} data from Jinhae Bay. Therefore, further work should be done to assess the atmospheric correction results of the GOCI R_{rs} data at the blue bands based on *in situ* R_{rs} measurements from Jinhae Bay. Such assessments would enable the development of new atmospheric correction algorithms optimized for coastal waters, perhaps including algorithms based on a multilayer neural network (Fan et al., 2017), with the final objective of developing a regionally optimized Chl-a algorithm for the GOCI R_{rs} products in Jinhae Bay. Raman scattering effects may also need to be considered to develop regional Chl-a algorithms because Raman fractions can contribute $\sim 8\%$ in R_{rs} at 555 nm in Case-2 waters (Gupta, 2015). These future works will thus yield a more accurate refinement of our GOCI-derived approach.

CONCLUSION

In order to provide a baseline approach to satellite-based coastal monitoring of the eutrophic Jinhae Bay environment in near real-time, we compared the GOCI-derived Chl-a estimates from two global open ocean algorithms and four regional algorithms with *in situ* Chl-a measurements between 2011 and 2016. Among the six tested ocean color algorithms, the YOC algorithm yielded the best performance results, producing Chl-a estimates closer to the 1:1 line compared to the other algorithms and spatial patterns similar to the *in situ* Chl-a values. Time series analyses of the *in situ* and GOCI-derived Chl-a values also agreed well, with the YOC algorithm detecting seasonal variations similar to those measured. Although the GOCI-derived Chl-a values from YOC algorithm showed the best fit to the *in situ* values from Jinhae Bay, this algorithm nonetheless yielded biased estimates

(e.g., a slight underestimation of high *in situ* Chl-a values $> \sim 1.0 \text{ mg m}^{-3}$). Hence, a Chl-a algorithm regionally optimized for Jinhae Bay must be further developed by collecting *in situ* R_{rs} data, which would enhance the opportunity to monitor eutrophication associated with anthropogenic activities in near real-time across Jinhae Bay by providing a more accurate Chl-a estimation.

AUTHOR CONTRIBUTIONS

J-EY and I-NK developed the idea and wrote the manuscript. J-EY, J-HL, SS, S-HY, H-JO, J-DH, J-IK, and S-SK conducted the literature survey and analysis. All the authors discussed and approved the final manuscript.

ACKNOWLEDGMENTS

This work was supported by Research on the characteristics of marine ecosystem and oceanographic observation in Korean waters (R2019041). This research was a part of the project titled Improvements of ocean prediction accuracy using numerical modeling and artificial intelligence technology, funded by the Ministry of Oceans and Fisheries, Korea. This work was also supported by the National Research Foundation of Korea (NRF) grant funded by the Korea government (MSIT) (NRF-2019R1F1A1051790). Thanks to the KOSC staff and NASA's Ocean Biology Processing Group for providing GOCI data used in this study.

SUPPLEMENTARY MATERIAL

The Supplementary Material for this article can be found online at: <https://www.frontiersin.org/articles/10.3389/fmars.2019.00359/full#supplementary-material>

REFERENCES

- Ahn, J.-H., Park, Y.-J., and Fukushima, H. (2018). Comparison of aerosol reflectance correction schemes using two near-infrared wavelengths for ocean color data processing. *Remote Sens.* 10:1791. doi: 10.3390/rs10111791
- Ahn, J.-H., Park, Y.-J., Kim, W., and Lee, B. (2016). Simple aerosol correction technique based on the spectral relationships of the aerosol multiple-scattering reflectances for atmospheric correction over the oceans. *Opt. Express.* 24, 29659–29669. doi: 10.1364/OE.24.029659
- Ahn, J.-H., Park, Y.-J., Kim, W., Lee, B., and Oh, I. S. (2015). Vicarious calibration of the geostationary ocean color imager. *Opt. Express.* 23, 23236–23258. doi: 10.1364/OE.23.023236
- Ahn, J.-H., Park, Y.-J., Ryu, J. H., Lee, B., and Oh, I. S. (2012). Development of atmospheric correction algorithm for Geostationary *Ocean Sci. J.* 47, 247–259. doi: 10.1007/s12601-012-0026-2
- Amante, C., and Eakins, B. W. (2009). *ETOPO1 1 Arc-Minute Global Relief Model: Procedures, Data Sources and Analysis*. NOAA Technical Memorandum NESDIS NGDC-24. National Geophysical Data Center, NOAA.
- Bae, H., Lee, J.-H., Song, S. J., Park, J., Kwon, B.-O., Hong, S., et al. S. (2017). Impacts of environmental and anthropogenic stresses on macrozoobenthic communities in Jinhae Bay, Korea. *Chemosphere* 171, 681–691. doi: 10.1016/j.chemosphere.2016.12.112
- Baek, S.-H., Son, M., Hyun, B.-G., Kim, D.-S., Choi, H.-W., and Kim, Y.-O. (2012). The correlation between environmental factors and phytoplankton communities in spring and summer stratified water-column at Jinhae Bay, Korea. *Korean J. Environ. Biol.* 30, 219–230.
- Baek, S. H., and Kim, Y. O. (2010). The Study of summer season in Jinhae Bay-Short-term changes of community structure and horizontal distribution characteristics of phytoplankton. *Korean J. Environ. Biol.* 28, 115–124.
- Bailey, S. W., Franz, B. A., and Werdell, P. J. (2010). Estimation of near-infrared water-leaving reflectance for satellite ocean color data processing. *Optics Express* 18, 7521–7527. doi: 10.1364/OE.18.007521
- Bailey, S. W., and Werdell, P. J. (2006). A multi-sensor approach for the on-orbit validation of ocean color satellite data products. *Remote Sens. Environ.* 102, 12–23. doi: 10.1016/j.rse.2006.01.015
- Bukata, R. P., Jerome, J. H., Kondratyev, A. S., and Pozdnyakov, D. V. (1995). *Optical Properties and Remote Sensing of Inland and Coastal Waters*. Boca Raton, FL: CRC Press.
- Cho, H.-Y., and Chae, J.-W. (1998). Analysis on the Characteristics of the Pollutant Load in Chinhae-Masan Bay. *Korean Soc. Coast. Ocean Eng.* 10, 132–140.
- Cho, H. Y., Chae, J. W., and Chun, S. Y. (2002). Stratification and DO concentration change in Chinhae-Masan Bay. *J. Korean Soc. Coast. Ocean Eng.* 14, 295–307.
- Cho, K.-J., Choi, M.-Y., Kwak, S.-K., Im, S.-H., Kim, D.-Y., Park, J., et al. (1998). Eutrophication and seasonal variation of water quality in masan-Jinhae Bay. *Sea* 3, 193–202.
- Cho, S., Ahn, Y. H., Ryu, J. H., Kang, G.-S., and Youn, H.-S. (2010). Development of Geostationary Ocean Color Imager (GOCI). *Korean J. Remote Sens.* 26, 157–165.
- Choi, J.-K., Park, Y. J., Ahn, J. H., Lim, H.-S., Eom, J., and Ryu, J.-H. (2012). GOCI, the world's first geostationary ocean color observation satellite, for the monitoring of temporal variability in coastal water turbidity. *J. Geophys. Res. Oceans* 117:C09004. doi: 10.1029/2012JC008046
- Fan, Y., Li, W., Gatebe, C. K., Jamet, C., Zibordi, G., Schroeder, T., et al. (2017). Atmospheric correction and aerosol retrieval over coastal waters using multilayer neural networks. *Remote Sens. Environ.* 199, 218–240. doi: 10.1016/j.rse.2017.07.016
- Garcia, C. A. E., Garcia, V. M. T., and McClain, C. R. (2005). Evaluation of SeaWiFS chlorophyll algorithms in the Southwestern Atlantic and Southern Oceans. *Remote Sens. Environ.* 95, 125–137. doi: 10.1016/j.rse.2004.12.006
- Gitelson, A., Karniel, A., Goldman, N., Yacobi, Y. Z., and Mayo, M. (1996). Chlorophyll estimation in the Southeastern Mediterranean using CZCS images: adaptation of an algorithm and its validation. *J. Mar. Syst.* 9, 283–290. doi: 10.1016/S0924-7963(95)00047-X
- Glover, D. M., Jenkins, W. J., and Doney, S. C. (2011). *Modeling Methods for Marine Science*. Cambridge, UK: Cambridge University Press.
- Gordon, H. R., and Wang, M. (1994). Retrieval of water-leaving radiance and aerosol optical thickness over the oceans with SeaWiFS: a preliminary algorithm. *Appl. Opt.* 33, 443–452. doi: 10.1364/AO.33.000443
- Gordon, H. Y., and Morel, A. (1983). “Remote assessment of ocean color for interpretation of satellite visible imagery: a review,” in *Lecture Notes on Coastal and Estuarine Studies*, eds R. T. Barber, M. J. Bowman, C. N. K. Mooers et al. (New York, NY: Springer Verlag), 1–144. doi: 10.1029/LN004
- Grasshoff, K. (1983). “Determination of nitrate,” in *Methods of Seawater Analysis. Second, Revised and Extended Edition*, eds K. Grasshoff, M. Ehrhardt, and K. Kremling (Weinheim: Verlag Chemie).
- Gupta, M. (2015). Contribution of Raman scattering in remote sensing retrieval of suspended sediment concentration by empirical modeling. *IEEE J. Sel. Top. Appl. Earth Obs. Remote Sens.* 8, 398–405. doi: 10.1109/JSTARS.2014.2361336
- Hattab, T., Jamet, C., Sammari, C., and Lahbib, S. (2013). Validation of chlorophyll- α concentration maps from Aqua MODIS over the Gulf of Gabes (Tunisia): comparison between MedOC3 and OC3M bio-optical algorithms. *Int. J. Remote Sens.* 34, 7163–7177. doi: 10.1080/01431161.2013.815820
- Holmes, R. W. (1970). The secchi disk in turbid coastal waters. *Limnol. Oceanogr.* 15, 688–694. doi: 10.4319/lo.1970.15.5.00688
- Hooker, S., and McClain, C. (2000). The calibration and validation of SeaWiFS data. *Prog. Oceanogr.* 45, 427–465. doi: 10.1016/S0079-6611(00)00012-4
- IOCCG (2000). “Remote sensing of ocean colour in coastal, and other optically-complex, waters,” in *Reports of the International Ocean-Colour Coordinating Group*, ed S. Sathyendranath (Dartmouth: IOCCG).
- IOCCG (2010). “Atmospheric correction for remotely-sensed ocean-colour products,” in *Reports of International Ocean-Colour Coordinating Group*, ed M. Wang (Dartmouth: IOCCG).
- Jeong, K. S., Cho, J. H., Lee, J. H., and Kim, K. H. (2006). Accumulation history of anthropogenic heavy metals (cu, zn, and pb) in masan bay sediments, southeastern korea: a role of chemical front in the water column. *Geosci. J.* 10, 445–455. doi: 10.1007/BF02910438
- Kang, S. W. (1991). Circulation and pollutant dispersion in Masan-Jinhae Bay of Korea. *Mar. Pollut. Bull.* 23, 37–40. doi: 10.1016/0025-326X(91)90646-A
- Kim, D., Baek, S. H., Yoon, D. Y., Kim, K.-H., Jeong, J.-H., Jang, P.-G., et al. (2014). Water quality assessment at Jinhae Bay and Gwangyang Bay, South Korea. *Ocean Sci. J.* 49:251. doi: 10.1007/s12601-014-0026-5
- Kim, D., Choi, H. W., Choi, S. H., Baek, S. H., Kim, K. H., Jeong, J. H., et al. (2013). Spatial and seasonal variations in the water quality of Jinhae Bay, Korea. *N. Z. J. Mar. Freshwater Res.* 47, 192–207. doi: 10.1080/00288330.2013.772066
- Kim, D., Lee, C.-W., Choi, S.-H., and Kim, Y. O. (2012). Long-term changes in water quality of Masan Bay, Korea. *J. Coast. Res.* 2012, 923–929. doi: 10.2112/JCOASTRES-D-11-00165.1
- Kim, N. S., Kang, H., Kwon, M.-S., Jang, H.-S., and Kim, J. G. (2016). Comparison of seawater exchange rate of small scale inner bays within Jinhae Bay. *J. Korean Soc. Mar. Environ. Energy* 19, 74–85. doi: 10.7846/JKOSMEE.2016.s19.1.74
- Kim, S.-Y., Lee, Y.-H., Kim, Y.-S., Shim, J.-H., Ye, M.-J., Jeon, J.-W., et al. (2012). Characteristics of marine environmental in the hypoxic season at Jinhae Bay in 2010. *Korea J. Nat. Conserv.* 6, 115–129. doi: 10.11624/KJNC.2012.6.2.115
- Kim, W., Moon, J.-E., Park, Y.-J., and Ishizaka, J. (2016). Evaluation of chlorophyll retrievals from Geostationary Ocean Color Imager (GOCI) for the North-East Asian region. *Remote Sens. Environ.* 184, 482–495. doi: 10.1016/j.rse.2016.07.031
- Kim, Y.-S., Lee, Y.-H., Kwon, J.-N., and Choi, H.-G. (2015). The effect of low oxygen conditions on biogeochemical cycling of nutrients in a shallow seasonally stratified bay in southeast korea (jinhae bay). *Mar. Pollut. Bull.* 95, 333–341. doi: 10.1016/j.marpolbul.2015.03.022
- Knap, A., Michaels, A., Close, A., Ducklow, H., and Dickson, A. (1996). *Protocols for the Joint Global Ocean Flux Study (JGOFS) Core Measurements*. JGOFS Report Nr. 19, 170pp. Reprint of the IOC Manuals and Guides No. 29, UNESCO 1994.
- Kwak, S.-K., Choi, M. Y., and Cho, K.-J. (2001). Distribution and occurrence frequency of red-tide causing flagellates in the Masan-Jinhae Bay. *Algae* 16, 315–323.
- Laws, E. A., and Archie, J. W. (1981). Appropriate use of regression analysis in marine biology. *Mar. Biol.* 65, 13–16. doi: 10.1007/BF00397062

- Lee, C., and Lim, W. (2006). Variation of harmful algal blooms in Masan-Chinhae Bay. *ScienceAsia* 32(Suppl. 1), 51–56. doi: 10.2306/scienceasia1513-1874.2006.32(s1).051
- Lee, C.-W., and Min, B.-Y. (1990). Pollution in Masan Bay, a matter of concern in South Korea. *Mar. Pollut. Bull.* 21, 226–229. doi: 10.1016/0025-326X(90)90338-9
- Lee, H. J., Wang, Y. P., Chu, Y. S., and Jo, H. R. (2006). Suspended sediment transport in the coastal area of Jinhae Bay—Nakdong Estuary, Korea Strait. *J. Coast. Res.* 225, 1062–1069. doi: 10.2112/04-0231.1
- Lee, J., Kim, S.-G., and An, S. (2017). Dynamics of the physical and biogeochemical processes during hypoxia in Jinhae Bay, South Korea. *J. Coast. Res.* 33, 854–863. doi: 10.2112/JCOASTRES-D-16-00122.1
- Lee, J., Park, K.-T., Lim, J.-H., Yoon, J.-E., and Kim, I.-N. (2018). Hypoxia in korean coastal waters: a case study of the natural Jinhae Bay and Artificial Shihwa Bay. *Front. Mar. Sci.* 5:70. doi: 10.3389/fmars.2018.00070
- Lim, H.-S., Diaz, R. J., Hong, J.-S., and Schaffner, L. C. (2006). Hypoxia and benthic community recovery in Korean coastal waters. *Mar. Pollut. Bull.* 52, 1517–1526. doi: 10.1016/j.marpolbul.2006.05.013
- Lim, J.-H., Lee, S. H., Park, J., Lee, J., Yoon, J.-E., and Kim, I.-N. (2018). Coastal Hypoxia in the Jinhae Bay, South Korea: mechanism, spatiotemporal variation, and implications (based on 2011 survey). *J. Coast. Res.* 85, 1481–1485. doi: 10.2112/SI85-297.1
- Moon, H.-B., Yoon, S.-P., Jung, R.-H., and Choi, M. (2008). Wastewater treatment plants (WWTPs) as a source of sediment contamination by toxic organic pollutants and fecal sterols in a semi-enclosed bay in Korea. *Chemosphere* 73, 880–889. doi: 10.1016/j.chemosphere.2008.07.038
- Moon, J.-E., Ahn, Y.-H., Ryu, J.-H., and Shanmugam, P. (2010). Development of ocean environmental algorithms for Geostationary Ocean Color Imager (GOCI). *Korean J. Remote Sens.* 26, 189–207.
- Moon, J.-E., Park, Y.-J., Ryu, J.-H., Choi, J.-K., Ahn, J.-H., Min, J.-E., et al. (2012). Initial validation of GOCI water products against *in situ* data collected around Korean peninsula for 2010–2011. *Ocean Sci. J.* 47, 261–277. doi: 10.1007/s12601-012-0027-1
- Morel, A., and Prieur, L. (1977). Analysis of variations in ocean color. *Limnol. Oceanogr.* 22, 709–722. doi: 10.4319/lo.1977.22.4.0709
- NASA (2010). *Ocean Color Chlorophyll (OC)* v6. Available online at: <https://oceancolor.gsfc.nasa.gov/reprocessing/r2009/ocv6/>
- NIFS (2012). *Annual Report of Marine Environment Monitoring Around Aquaculture Area in Korea*. National Institute of Fisheries Science, Busan.
- NIFS (2013). *Annual Report of Marine Environment Monitoring Around Aquaculture Area in Korea*. National Institute of Fisheries Science, Busan.
- NIFS (2014). *Annual Report of Marine Environment Monitoring Around Aquaculture Area in Korea*. National Institute of Fisheries Science, Busan.
- NIFS (2015). *Annual Report of Marine Environment Monitoring Around Aquaculture Area in Korea*. National Institute of Fisheries Science, Busan.
- NIFS (2016). *Annual Report of Marine Environment Monitoring Around Aquaculture Area in Korea*. National Institute of Fisheries Science, Busan.
- NIFS (2017). *Annual Report of Marine Environment Monitoring Around Aquaculture Area in Korea*. National Institute of Fisheries Science, Busan.
- O'Reilly, J. E., Maritorena, S., O'Brien, M., Siegel, D., Toole, D., Menzies, D., et al. (2000). SeaWiFS postlaunch calibration and validation analyses, part 3. *NASA Tech. Memo* 206892:11.
- Park, K.-W., Suh, Y.-S., and Lim, W.-A. (2012). Seasonal Changes in Phytoplankton Composition in Jinhae Bay, 2011. *J. Korean Soc. Mar. Environ. Saf.* 18, 520–529. doi: 10.7837/kosmes.2012.18.6.520
- Park, S. C., Lee, K. W., and Song, Y. I. (1995). Acoustic characters and distribution pattern of modern fine-grained deposits in a tide-dominated coastal bay: Jinhae bay, southeast korea. *Geo-Mar. Lett.* 15, 77–84. doi: 10.1007/BF01275410
- Pitarch, J., Volpe, G., Colella, S., Krasemann, H., and Santolieri, R. (2016). Remote sensing of chlorophyll in the Baltic Sea at basin scale from 1997 to 2012 using merged multi-sensor data. *Ocean Sci.* 12, 379–389. doi: 10.5194/os-12-379-2016
- Pradhan, Y., Thomaskutty, A. V., Rajawat, A. S., and Shailesh, N. (2005). Improved regional algorithm to retrieve total suspended particulate matter using IRS-P4 ocean colour monitor data. *J. Opt. A Pure Appl. Opt.* 7, 343. doi: 10.1088/1464-4258/7/7/012
- Ruddick, K. G., Gons, H. J., Rijkeboer, M., and Tilstone, G. (2001). Optical remote sensing of chlorophyll a in case 2 waters by use of an adaptivetwo-band algorithm with optimal error properties. *Appl. Opt.* 40, 3575–3585. doi: 10.1364/AO.40.003575
- Ryu, J. H., Choi, J. K., Eom, J., and Ahn, J.-H. (2011). Temporal variation in Korean coastal waters using Geostationary Ocean Color Imager. *J. Coast Res.* 64, 1731–1735.
- Ryu, S.-H., Lee, I.-C., and Jin, S.-H. (2018) Analysis of annual variation of water quality and fisheries production in Jinhae Bay, Korea. *J. Kor. Soc. Fish Mar. Edu.* 30, 1215–1222. doi: 10.13000/JFMSE.2018.08.30.1215
- Sarangi, R. K., Chauhan, P., and Nayak, S. R. (2002). Vertical diffuse attenuation coefficient (Kd) based optical classification of IRS-P3 MOS-B satellite ocean colour data. *J. Earth Syst. Sci.* 111, 237–245. doi: 10.1007/BF02701970
- Siswanto, E., Tang, J., Yamaguchi, H., Ahn, Y.-H., Ishizaka, J., Yoo, S., et al. (2011). Empirical ocean-color algorithms to retrieve chlorophyll-a, total suspended matter, and colored dissolved organic matter absorption coefficient in the Yellow and East China Seas. *J. Oceanogr.* 67:627. doi: 10.1007/s10872-011-0062-z
- Tassan, S. (1994). Local algorithms using SeaWiFS data for the retrieval of phytoplankton, pigments, suspended sediment, and yellow substance in coastal waters. *Appl. Opt.* 33, 2369–2378. doi: 10.1364/AO.33.002369
- Tilstone, G. H., Lotliker, A. A., Miller, P. I., Ashraf, P. M., Kumar, T. S., Suresh, T., et al. (2013). Assessment of MODIS-Aqua chlorophyll-a algorithms in coastal and shelf waters of the eastern Arabian Sea. *Cont. Shelf Res.* 65, 14–26. doi: 10.1016/j.csr.2013.06.003
- U.S. EPA. (1997a). *Method 445.0: In vitro Determination of Chlorophyll a and Pheophytin a in Marine and Freshwater Algae by Fluorescence*. National Exposure Research Laboratory, Office of Research and Development, USEPA, Cincinnati, OH.
- U.S. EPA. (1997b). *Method 353.4: Determination of Nitrate and Nitrite in Estuarine and Coastal Waters by Gas Segmented Continuous Flow Colorimetric Analysis*. National Exposure Research Laboratory, Office of Research and Development, USEPA, Cincinnati, OH.
- Vaicute, D., Bresciani, M., and Bucas, M. (2012). Validation of MERIS bio-optical products with *in situ* data in the turbid Lithuanian Baltic Sea coastal waters. *J. Appl. Remote Sens.* 6:063568. doi: 10.1117/1.JRS.6.063568
- Welschmeyer, N. A. (1994). Fluorometric analysis of chlorophyll a in the presence of chlorophyll b and pheophytins. *Limnol. Oceanogr.* 39, 1985–1992. doi: 10.4319/lo.1994.39.8.1985
- York, D. (1966). Least-squares fitting of a straight line. *Can. J. Phys.* 44, 1079–1086. doi: 10.1139/p66-090
- Zhang, M., Tang, J., Dong, Q., Song, Q., and Ding, J. (2010). Retrieval of total suspended matter concentration in the Yellow and East China Seas from MODIS imagery. *Remote Sens. Environ.* 114, 392–403. doi: 10.1016/j.rse.2009.09.016

Conflict of Interest Statement: The authors declare that the research was conducted in the absence of any commercial or financial relationships that could be construed as a potential conflict of interest.

Copyright © 2019 Yoon, Lim, Son, Youn, Oh, Hwang, Kwon, Kim and Kim. This is an open-access article distributed under the terms of the Creative Commons Attribution License (CC BY). The use, distribution or reproduction in other forums is permitted, provided the original author(s) and the copyright owner(s) are credited and that the original publication in this journal is cited, in accordance with accepted academic practice. No use, distribution or reproduction is permitted which does not comply with these terms.